VALidation and Improvement of Airframe Noise prediction Tools (ACP8-GA-2009-233680)

Deliverable D38

WP 1

"Final Publishable Summary Report"

VALIANT is a Collaborative Project addressing the external noise challenges raised by the development of green aircrafts. VALIANT focuses on broadband airframe noise (AFN) by tackling both landing gears and high lift devices, which are the two main contributors to AFN of an aircraft at approach. The objective is to contribute to the ACARE strategic goal of reducing the external noise by 10 EPNdB per operation in 2020, taking 2001 as the baseline. European aeronautical industry has committed to meet this extremely demanding challenge. Amongst various other important aspects, the fulfilment of the ACARE objectives involves the improvement of accurate and fast prediction techniques to enable virtual prototyping and shorten development cycles. The consortium is very much aware of the fact that a project dealing with a real airframe with slat, flap and landing gear integrated in a unique complex geometry would not permit to answer the questions concerning the maturity and validation of the numerical methods. Indeed, such assembly would require prohibitive computations as well as wind tunnel testing, which are incompatible with the development, systematic comparison and experimental validation of high-accuracy numerical tools. This knowledge can be accumulated only by studying isolated generic configurations (slat, flap, landing gear, etc.). Moreover, previous and currently running research programs dealing with AFN, such as RAIN, SILENCE(R), AWIATOR, TIMPAN, CLEANSKY and OPENAIR, study realistic rather than generic configurations, with a clear focus on noise reduction technologies at realistic scale level. VALIANT is rather aiming at validating / improving noise prediction tools, representing a very complementary contribution towards the ACARE goals.

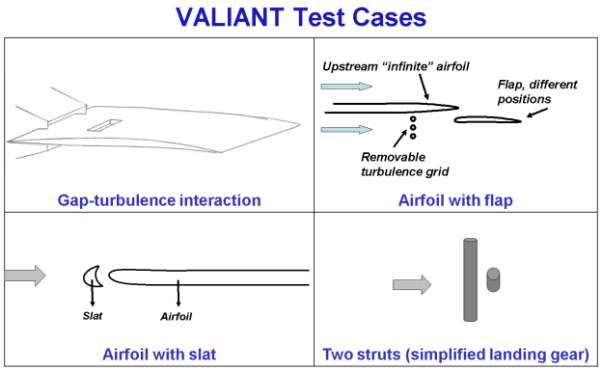

Figure 1: VALIANT test cases

Four specific flow configurations revealing the basic mechanisms of AFN generated by the most relevant elements of a real aircraft are selected in VALIANT for a thorough investigation aimed at validating and improving the broadband AFN predictive tools: gap turbulence interaction, flap+wing configuration, slat+wing configuration, two struts (Figure 1).

Having generic configurations permits to establish very complete and accurate experimental databases that can be used for the unambiguous validation of the prediction tools, which is an essential step towards their improvement. The first half of the project was thus focusing on measurements, especially to obtain the necessary measured data for the simulations, and on the first-pass simulations. Since numerical simulations (especially LES and DES) are very sensitive to boundary conditions, some measurements providing these inputs had to be conducted in the early stage of the project to permit a timely start of the simulation work. The second half of the project was focusing the theoretical developments of flap noise prediction, as well as the improvements of the existing tools based on the experiences gained through the first pass simulations. The last part of the project finalized all the developments and demonstrated their effect on the noise predictions.

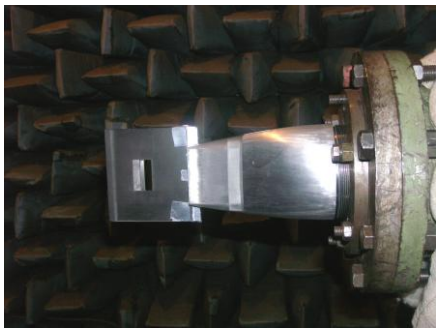

Figure 2: The gap model installed in the anechoic chamber AK-2 of TsAGI.

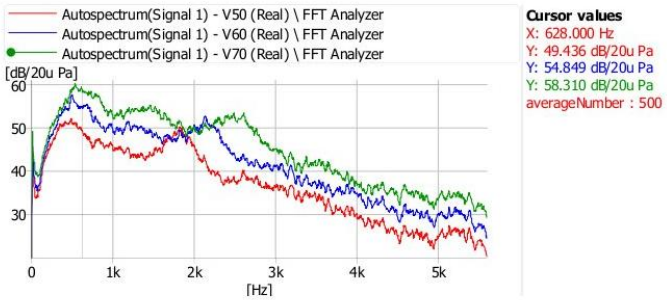

Figure 3: Comparison of autospectra for the different flow velocities V=50, 60,70 m/s; the model with gap, L=10 mm

All planned measurements related to the gap test case were performed by TsAGI (Figure 2). In the test matrix the gap width and the flow velocity was the main parameters to change. Besides, in addition to the data specified in the test matrix (different flow velocities and gap widths) some additional test cases were studied and additional characteristics have been measured (Figure 3) such as the correlations between the microphones which are expected to be useful in evaluation of the results of the numerical calculations performed for this test case.

The performed experimental work has resulted in a database, which includes

- time microphone signals processed in Pa;
- mean velocity and turbulence intensity profiles;
- time series of the velocities acquired from the hot wire measurements;
- Sound Pressure Levels in narrow bands with the smallest frequency resolution of 4 Hz achievable while maintaining a good averaging of the spectra;
- Sound Pressure Levels in frequency bands compatible with the frequency resolution achieved from the simulation (4 Hz).

Based on the inflow parameters provided by these measurements the numerical partners were able to perform their state-of-the-art simulations on this geometry (Figure 4). LES-based approaches (combined with FW-H acoustic propagation) provide reasonable results, but are particularly tedious in terms of CPU and memory needs. Indeed, a long simulation period is needed to smooth the spectra and large unsteady data have to be stored for the acoustic propagation. IMM performed simulations using the DES and DDES approaches, while TUB used just the DDES model. The numerical techniques used by the partners for implementing the DDES model, and, correspondingly, the codes differed from each others. TUB used the multi-block structured mesh and the hybrid scheme based on the switching between the 2nd and 3rd order schemes in LES/RANS regions. IMM used the tetrahedral mesh and the hybrid scheme with switching from 6th to 5th order schemes.

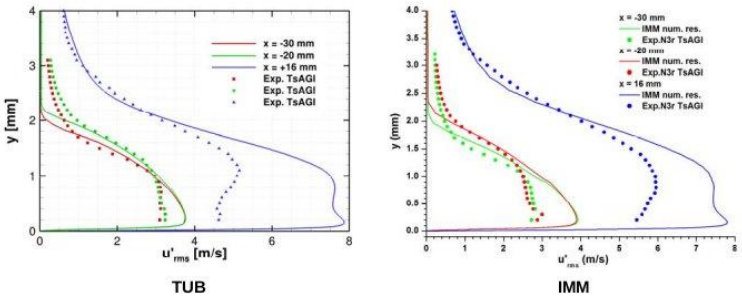

Figure 4: Time-averaged velocity fluctuations from DDES compared to experimental data from TsAGI.

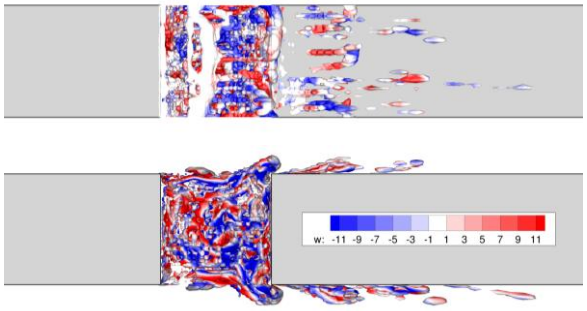

Figure 5: Vortical structures captured in the gap configuration, indicated by λ_2-isosurface coloured with spanwise velocity component.

The numerical results obtained by the "numerical" partners (TUB and IMM) are in a quite good agreement with each other. This fact testifies in a good verification and applicability of the numerical techniques in use. It turned out that the characteristics of the incoming turbulent boundary layer has a significant effect on the source generation, and such way, indirectly on the far-field noise prediction.

At the same time, the deviation of both numerical results from the experimental data of TsAGI seems, though not crucial, but still significant. In particular, the discrepancy in peak frequencies is 21% and 26% in cases of TUB and IMM respectively. From the general standpoint, there may be two potential reasons of the difference between the numerical and experimental results.

First, the results may differ due to the inconsistency in the case set-up:

- For instance, the numerical partners assumed the uniform upstream flow in the whole domain, while TsAGI used the round jet placing the plate inside the core region.
- In the experimental case, the plate was of finite length and the shedding from the trailing edge contributed to the far field while the computational set-up was based on the infinite plate.
- The gap width (in span-wise direction) in the simulations is only 1/8 of the experimental gap width.
- The farfield results were then corrected using the Kato correction as it is in the fully uncorrelated case. The latter can also introduce errors since the possible correlation should be carefully taken into account at the rescaling.

Second, since both TUB and IMM teams applied the same approach to the turbulent flow simulation, the DDES model may appear not in a full measure appropriate for the gap-turbulence interaction case.

The wing-flap simulations measurements were done in the anechoic wind tunnel of ECL. Investigations of several wing-flap arrangements have been performed during the tests. During the two measurement campaigns detailed acoustic and aerodynamic data were collected by ECL and ONERA (wall-pressure, hot-wire, microphone array, single microphone measurements).

Figure 6: Onera's microphone antenna in ECL's wind tunnel

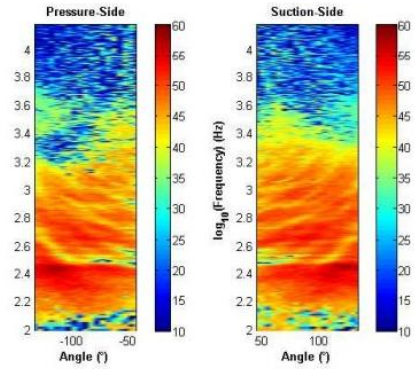

Figure 7: Flap-noise radiation map, turbulent inflow, 50m/s, in-line configuration

The mock-up design ensures a negligible mean lift and the associated nearly parallel flow, more convenient because free of jet-deflection issues. Considering non-lifting, bodies close to a flat-plate geometry also allows focusing on basic physical phenomena produced by a two-element system without additional distortions or gradients. Typically in such arrangements the scattering mechanisms are more clearly highlighted. The preliminary analysis made on the two selected configurations of a tandem with no overlap and an overlapping system provides a first view of the source and scattering mechanisms. For instance, the radiation maps feature both the sound-generating mechanisms by the frequency content and noise levels, on the one hand, and the scattering properties through the interference patterns and the asymmetry of the cartography.

In the second half of the project, all the partners involved in this task performed both the first-pass and the improved simulations. In addition to a pure self-noise test case without the flap two interaction-noise test cases with the flap located either behind or below the wing have been investigated within this task. DLR, NTS and VKI performed nearfield simulations of the turbulent flow fields around these configurations. Based on the unsteady flow field data acquired, several farfield noise predictions have been carried out by DLR, NTS, LMS and TUB. Both nearfield and farfield results were compared to experimental data, which was provided by ECL.

Three different numerical methods have been employed by the teams involved in the nearfield simulations. The dominant sound sources were either directly represented through turbulence resolving incompressible LES (VKI) or compressible E-IDDES (NTS) or they were reconstructed based on time-averaged compressible RANS solutions of the turbulent mean flows using a synthetic RPM model (DLR). Additional modelling assumptions involved in the latter approach make it likely to be less accurate than the turbulence resolving approaches. However, since steady RANS simulations are naturally much cheaper than any scale resolving simulation, it is especially attractive through its reduced computational cost. In section 10, time-averaged wall pressures and velocity profiles obtained with the abovementioned approaches are juxtaposed for an average mean flow speed of 50 m/s allowing for an assessment of the individual approaches.

Since the results obtained with both compressible nearfield approaches are in much better agreement with the measurements than results obtained with the incompressible approach, it might be wrongly concluded that the turbulence representation is of less crucial importance than the incorporation of compressibility effects. However, the deviations seen for the incompressible LES are most probably caused by a too dissipative numerical method leading to an inaccurate turbulence representation and are not due to the limitation to constant density flows. Detailed cross-plotting allowed assessing the advantages and shortcomings of all the methods, while offering the insight of further improvements. The boundary layer along the wing is turbulent, what is

one of the key points of this simulation. In order to have a realistic turbulent boundary layer generated at the inlet, several approaches have been developed within the project (immersed boundary strip, synthetic turbulent inlet).

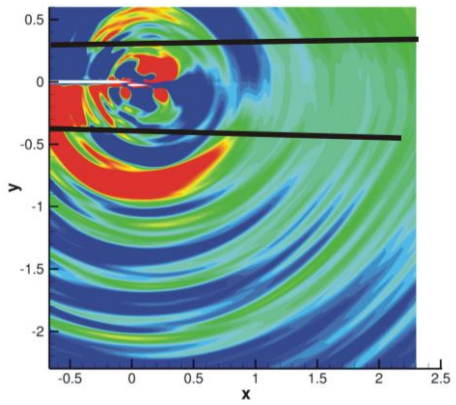

Figure 8: Superposition of individual snapshots of the sound pressure for different sources, for the wing-flap test case.

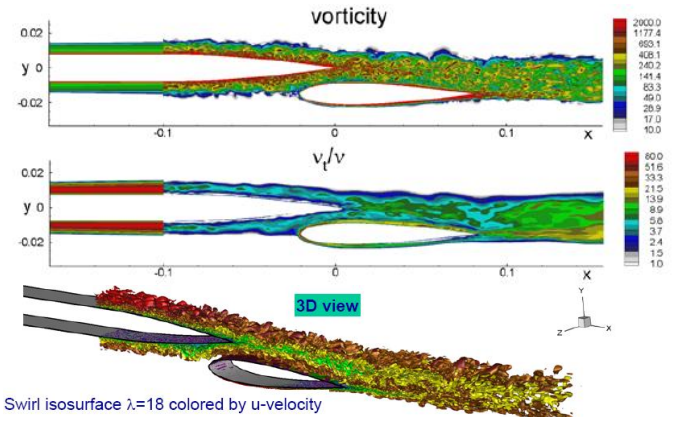

Figure 9: Visualization of E-IDDES solution for the wing-flap case: snapshots of vorticity and eddy viscosity in XY-plane and 3D view of swirl iso-surface.

As the turbulence is the source of the broadband noise generation, its correct representation in the nearfield simulation is a key ingredient for accurate noise predictions. Although the methods used by DLR, NTS, TUB and LMS for the farfield noise predictions were quite different, the individual results obtained with these methods were seen to be very close to each other when based on the same source data and also very similar in shape to the corresponding wall pressure spectra. In order to obtain the farfield pressure perturbations DLR has solved a source augmented set of Acoustic Perturbation Equations (APE), LMS used a Boundary Element Method (BEM) and both TUB and NTS employed an integral solution to the equation of Ffowcs-Williams and Hawkings (FWH), whereby the numerical solution was obtained in the time-domain or frequency-domain, respectively.

The agreement between numerical results obtained with the compressible approaches and the experimental data is quite good for time-averaged wall pressures, velocity-profiles and for the pressure spectra on the surfaces (except for RMP positions W20 and W224) and in the farfield as well. In general, the applied combinations of turbulence resolving or RANS+RPM based nearfield simulations with farfield extrapolations based on APE, BEM or the FWH equation proved capable to give very reasonable results for the test cases under consideration, provided that the turbulent noise sources are properly described.

Experiments were conducted at ECL on a slat-wing mock-up which profile was designed by ONERA. The geometrical angle of attack of 25° has been taken in the open-jet experiment to fit with the reference angle of 18° considered in the accompanying computations in infinite flow. Aerodynamic and far-field acoustic data have been recorded at various flow speeds and different angles of attack around the reference value. The post-processing is still in progress. Farfield acoustic spectra display tonal components at frequencies, which follow Strouhal laws with the velocity, but are independent of the airfoil angle-of-attack (although the tone amplitude decreases when the a.o.a. increases). The noise source localisation maps indicate that those peaks are generated by 2D mechanism distributed along the airfoil span, with strong levels of correlation. At this stage, there are two different physical mechanisms that may explain these peaks, without clear

evidence of one being the most probable (and also considering that both mechanisms could be present).

The first mechanism is linked to laminar effects. Due to the small scale of the model, the boundary layers on the slat suction side may remain laminar up to the slat upper and lower trailing edges, with Tollmien-Schlichting waves interacting with the trailing edges. As already mentioned, we tested a boundary layer tripping device of thickness 0.2 mm on the slat suction side, but only at the slat upper trailing edge, and not at the lower trailing edge. Additional fruitful insights on this question were brought through discussions with Michael Pott-Polenske, who supervised several tests at DLR/AWB with the F16 model (same slat and wing leading edge shapes as the VALIANT airfoil). It appeared that the same peaks were observed there, and several tests were achieved with tripping devices of various thicknesses located at the upper and lower slat trailing edges. The conclusions were that (i) the laminar/turbulent transition could not be obtained at the upper slat TE, whatever the position and thickness of the tripping and (ii) only a very thick tripping device (0.6 mm) located 10 mm upstream the lower TE was required to remove these peaks. However, such a massive device was assumed to deeply modify the flow in the slat cove region, so finally a compromise between the elimination of tones and the quality of the flow was chosen with a device of intermediate thickness 0.3 mm.

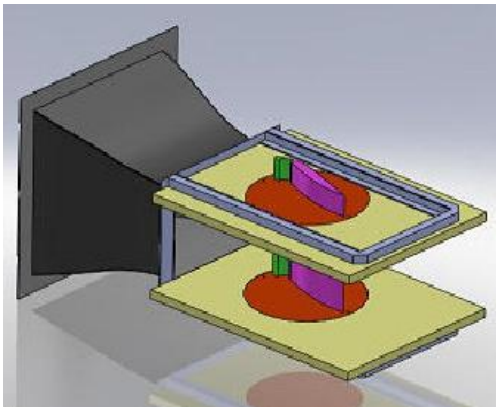

Figure 10: CAD-view of the experimental set-up (short bent section not shown). The disks can be rotated to vary the angle of attack.

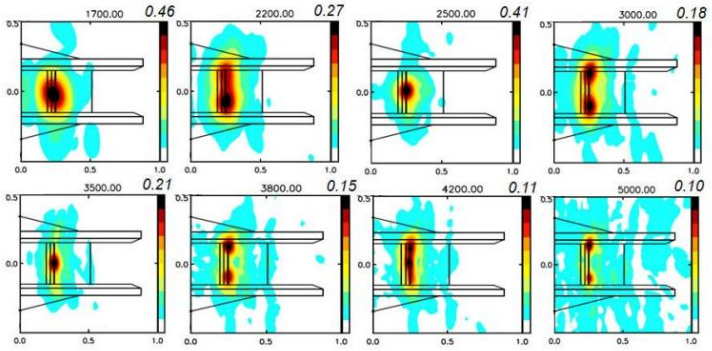

Figure 11: Airfoil with slat. Noise maps at incidence 25°. Each plot displays the frequency in Hz and the maximum level of correlation.

The second possible mechanism is that the slat cove may behave as a cavity subjected to a flow at grazing incidence, so the tones may be generated by Rossiter-like modes, characterized by a feedback loop between (i) the acoustic waves generated near the slat upper trailing edge by the impact of the shear layer generated at the slat lower trailing edge and (ii) the onset of vortices at the slat lower trailing edge. This hypothesis has been recently reinforced by a quantitative analysis based on the numerical simulation of the unsteady flow in the slat cove, performed by Onera in this project using LES in perturbation

The definition of the wing-slat case required a preliminary CFD and optimization step. ONERA performed a numerical optimization of the 2D airfoil-slat configuration, where the slat geometry is the Airbus FNG airfoil geometry F16 with a retracted wing-slat chord of 0.3 m. The objective was to get a mean flow and a distribution of noise sources in the slat region which is realistic with respect to a conventional high lift wing with deployed flap and slat and global incidence 4°, but with

minimizing the overall lift and deviation of the wind tunnel open-jet. The optimized airfoil is a 2-element wing with a nominal incidence of 18°. During the first 6th month meeting it was decided that the numerical teams can start with the configuration obtained by ONERA and the measurements have been adjusted to this 18° free-field configuration. Detailed numerical simulations including the whole test section revealed that the measurements should be conducted with an angle of attack 27° in order to reproduce the free stream conditions of 18°. The measurements conducted at ECL confirmed that an angle of attack of 25° permits to reproduce the targeted pressure distribution in the slat area. For CFD, VKI, ONERA, NTS conducted unsteady flow simulations based on LES-like methods. DLR and NUMECA used a stochastic approach of turbulence reconstruction from steady RANS computation as described before. It was found that the transient part of the simulations is very long, approximately 10 chord flow-through. As for the results, both the flow and the wall-pressure were captured well in the simulations, however, along the slat significant deviations were found. It is not clear at this point if it is due to the different angle of attack, or resulted by other numerical effect.

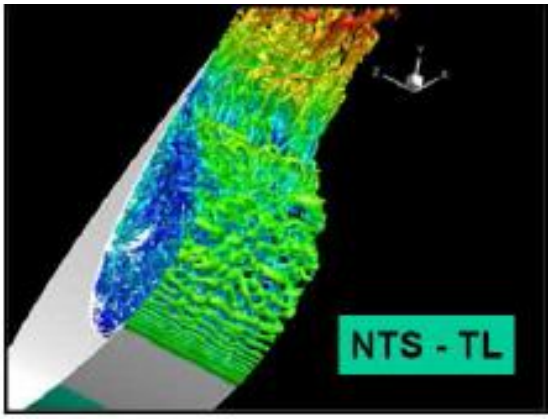

Figure 12: Q iso-surfaces in the slat-cove region to demonstrate the development of coherent structures in this region.

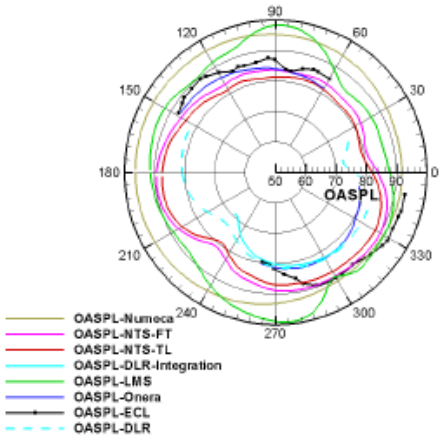

Figure 13: Comparison of the far-field sound directivity between the numerical partners and with the measurements.

The task coordinator provided requirements and guidelines for the partners to format their numerical results in preparation of the final cross-plotting of all numerical predictions against the experimental data. These cross-plotting are provided in the last section of this report, including static pressure coefficients, velocity surveys (mean/RMS), wall pressure PSD (Power Spectral Densities), and farfield acoustic pressure (PSD and OASPL). Although all prediction methods are globally in fair agreement with the experimental data, it appears that the simulations proposed by NTS show the best quantitative and qualitative agreement with the experimental data.

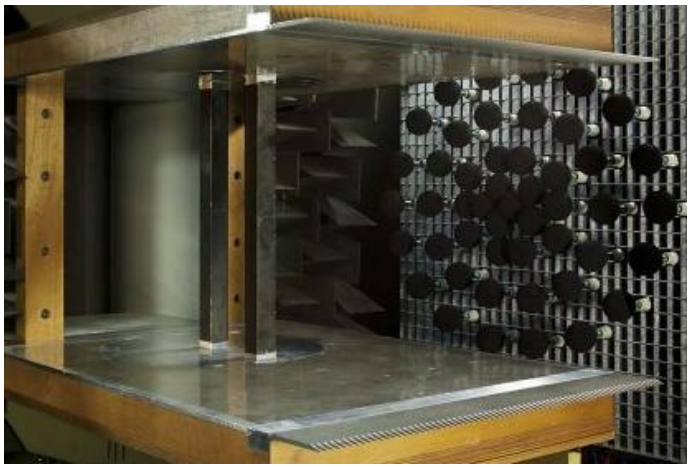

Figure 14: Two-struts set-up in KAT.

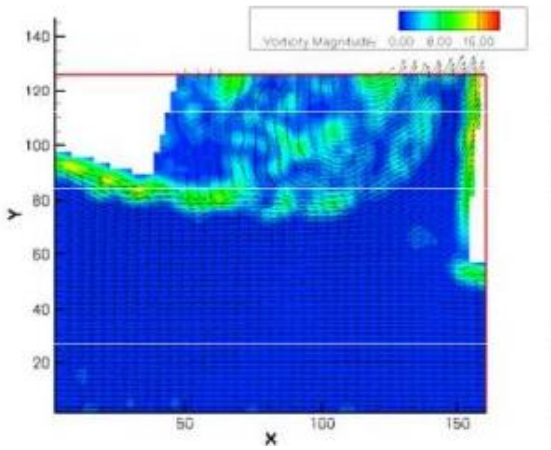

Figure 15:Instantaneous vorticity control by PIV measurements for benchmark configuration of -15°.

The two-struts configuration was measured in the small anechoic wind tunnel (KAT) of NLR. The objectives of these experiments were (1) to provide a benchmark database for the computations and (2) to obtain more insight in the basic noise generation mechanisms. In order to enable a thorough assessment of the numerical results NLR performed both far-field and microphone array measurements in order to determine the noise directivity and the source localization for different regimes of speeds and angles of attack of the two-struts alignment. Besides these acoustic measurements NLR obtained pressure data on the surfaces of the struts and VKI performed PIV measurements.

CIMNE, IMM, NUMECA and TUB performed numerical simulations on three distinct configurations of this test case, while NLR has been leading the experimental campaign. CIMNE has performed CFD simulations using a variational multi-scale technique. The inhomogeneous Helmholtz equation has been solved to compute the acoustic pressure in the far-field. IMM uses a hybrid Detached Eddy Simulation (DES) method for the numerical representation of the compressible viscous flow while the aeroacoustic analysis is based on the FW-H formulation. NUMECA has performed LES simulations and completed the aeroacoustic analysis based on the FW-H formulation. TUB performed the CFD simulations using a DDES technique and completed the aeroacoustic analysis based on the FW-H formulation.

Near-field and far-field results obtained by the different numerical partners have been extensively compared with experimental data. The computed time-averaged flow-fields are overall in good agreement with the experimental data. The discrepancies that are observed for some quantities (i.e. Cp values on the downstream side of the second strut, turbulent intensities between the two struts for the inclined configurations) are similar for all LES-based results (IMM, NUMECA TUB). This may be due to a systematical error in the numerical turbulence modeling. Alternatively, some of the deviations seen between experiment and simulation may be introduced through differing boundary conditions, e.g. effects of blockage, limited jet extent and/or endplates in the experiment are not reproduced in the simulations which assume a uniform flow.

The same post-processing approach has been used to evaluate near-field and far-field spectra from unsteady pressure signals. The dominant peaks in the solid-wall spectra are well captured for both struts with maximum discrepancies of about 5 dB in level and about 20 Hz in frequency. Again, the same discrepancies with respect to the experimental data are generally observed for all LES-based results. Since the simulated spanwise length is not the same as in the experiments, a

correction had to be applied to the computed far-field noise. This correction allows for some freedom in the choice of the numerical values for certain parameters. Even though more uncertainties are added through this correction, we noticed that the discrepancies for the far-field results with respect to the experimental data are not larger than the discrepancies observed for the solid-wall spectra.

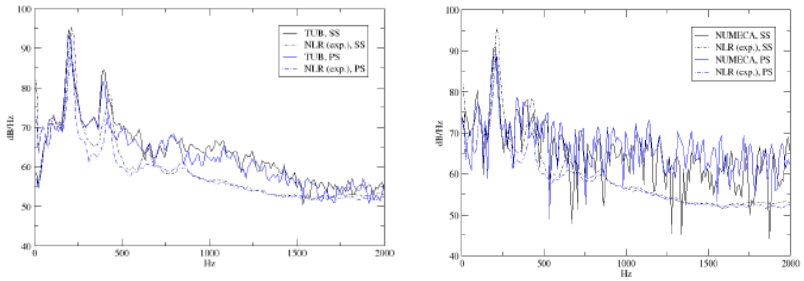

Figure 16: Comparison of the numerically obtained wall-pressure spectra (TUB and NUMECA) with measurements performed at NLR.

Figure 17: Q iso-surfaces demonstrate the flow topology for the two struts test case

In summary, LES-based approaches (combined with FW-H acoustic propagation) provide reasonable results, but are particularly tedious in terms of CPU and memory needs. Indeed, a long simulation period is needed to smooth the spectra and large unsteady data have to be stored for the acoustic propagation. Future research should focus on new technologies to reduce the CPU and memory requirements. The near-field results should first be improved with respect to the experimental data before comparing the far-field noise. For this purpose, the uncertainties in the experimental and numerical results should be critically assessed. In order to fine-tune the modelling approach, possible effects induced by the simplification of the modeled test case (effects of the end-plates, effects of limited jet extent, etc) should be investigated. An effective angle of attack could for example be used for a better match of the mean pressure distribution before comparing the emitted noise. Possible systematical errors in the turbulence modeling may be investigated by comparing the LES-based approaches to a DNS solution for a simple case.

The EU-Russia character of VALIANT, suggests that dissemination of the project achievements is an important priority. Inside the consortium, an open communication strategy was adopted. This is reached, in particular, by a strong interaction between the computational and experimental teams at all the project stages starting from the experiments set-up (guidelines for both experimental and numerical investigations) and ending by the collaborative analysis of the results of the simulations. The knowledge gained in the VALIANT project, namely the efficient and reliable numerical approaches to the AFN prediction, the insights into the noise mechanisms, and, last but not least, the experimental database accumulated during the project can be disseminated. It was decided in the closing meeting that the leaders of the experimental partners will take care of the data management of their measurements, while the Task leaders of the numerical setups will store the raw comparisons for further dissemination. Moreover, during the project detailed technical reports, publications in journals, presentations at national and international conferences, and also a rapid “penetration” of the gained new knowledge into the teaching courses have been given by many of the EU and Russian participants of the project at the national universities.

VALIANT project was expounded in the sixth European Aeronautics Days took place from 30th March to 1st April 2011 in Madrid. The conference brought together aeronautics stakeholders, ministries, agencies and R&D centers from all over Europe and overseas to network, presented their latest research results and discussed common future R&D projects enabling to show the mid-term status and the idea of VALIANT front of a huge audience.

In order to organize and manage the dissemination activities in an optimal manner, two different tasks are included in the project which address different ways of dissemination, namely, the exploitation plan and the dissemination of the technical information to the partners and interested third parties. In particular, the two open short courses on the basis of world-wide known platform of Lecture Series at VKI and the final project workshop, open for people and organisations from outside the consortium were an important channel to disseminate the project results. For each of these three events, a special invitation was sent to the scientists from other running EC projects. This helped to disseminate the information to the most interesting parties.

An efficient way of distributing the information and exchanging experimental and numerical data between the partners is a web site, including a restricted ftp site, which was updated according to need. This was especially helpful during the cross-comparison of numerical and experimental data.

In particular, the industrial partners will directly transfer the results of basic research and development into industrially applicable simulation methods and tools. After the end of the project the created and validated methods will be further explored on real (industrially relevant) problems in the daily work. The software vendors (NUMECA and the acoustics specialist company LMS) and SME's will benefit from the exploitation of the results of VALIANT by enhancement of their competitiveness on the international CFD-CAA market.

The research establishments participating in VALIANT could directly exploit the knowledge gained in the project by improving their numerical tools. Finally, the universities taking part in VALIANT incorporates the experience gained within the project into their research and into support of the industries they cooperate with. Also, as mentioned above, they can use the findings of VALIANT for teaching and training students and researchers.

Goal of the VALIANT project was to generate a validation database for airframe noise problems. It was decided by the consortium that this database is available for the public upon request. For more information please visit the project website: **www.cimne.com/websasp/valiant** or contact directly the project coordinator: Prof. Christophe Schram, **christophe.schram@vki.ac.be** **.**